View metadata, citation and similar papers at core.ac.uk
brought to you by CORE
provided by Apollo

A HIF2α-arginase axis is essential for the development of pulmonary hypertension

Andrew S. Cowburn, PhD[1,2]; Alexi Crosby, PhD[2]; David Macias, PhD[1]; Cristina Branco, PhD[1]; Renato Colaço, PhD[1]; Mark Southwood, PhD[3]; Laura E. Crotty Alexander, MD[4]; Nicholas W. Morrell, MD[2]; Edwin R. Chilvers, PhD[2]; and Randall S. Johnson, PhD[1,5]

Department of Physiology, Development and Neuroscience,[1] Department of Medicine,[2] University of Cambridge; Department of Pathology[3], Papworth Hospital NHS Foundation Trust; Division of Pulmonary and Critical Care, School of Medicine, University of California, San Diego,[4] Department of Cell and Molecular Biology, Karolinska Institute, Stockholm, Sweden[5]

For correspondence: Professor Randall S. Johnson, Department of Physiology, Development and Neuroscience, University of Cambridge, Downing Street, Cambridge. CB2 3EG. United Kingdom.

E-mail: rsj33@cam.ac.uk

Short title: HIF2α is essential for pulmonary hypertension

Keywords: HIF2α, arginase-1, pulmonary-endothelium, nitric oxide

Abstract

Pulmonary vasoconstriction initiates pulmonary vascular remodelling, which, when prolonged, leads to the development of pulmonary hypertension. The hypoxia-inducible transcription factors (HIFs), HIF-1α and HIF-2α, are known to contribute to the process of hypoxic pulmonary vascular remodelling. Here we show that HIF-2α, expressed in pulmonary endothelial cells, is essential for hypoxia-induced pulmonary arterial hypertension (PAH). Loss of endothelial HIF-2α expression prevented cardiac hypertrophy and vascular remodelling. A key target of HIF-2α in the endothelial cell is the arginase-1 enzyme, which directly influences vascular remodelling, and indirectly regulates nitric oxide synthesis. Deletion of arginase-1 in the pulmonary endothelium attenuated many of the pathophysiological symptoms associated with PAH, indicating that HIF-2α/arginase expression in endothelial cells is an essential feature of pulmonary hypertension. (word count 117)

Significance Statement

We show that the expression of the HIF-2α transcription factor in the endothelial cells of the lung is essential for the development of the pulmonary hypertension that results from prolonged exposure to low oxygen. We subsequently show that the HIF-2α transcription factors' control of the arginase-1 enzyme is required for the development of pulmonary hypertension, and of its resultant vascular remodelling. This shows that low oxygen levels cause a persistent expression, first, of HIF-2α, and then of arginase-1, which in turn regulates vascular constriction and the downstream changes in extracellular matrix formation; these are the fundamental characteristics of the pulmonary arterial hypertension syndrome.

Introduction

Hypoxia affects vascular flow in mammals in many different ways, but significant drops in oxygenation have a particular effect on the lung. In the pulmonary vascular bed, alveolar hypoxia leads to an immediate vasoconstrictor response (hypoxic pulmonary vasoconstriction, or HPV) (1). This effect is intended to preserve oxygen in the systemic circulation by reducing perfusion of regions of the lung with lowered levels of air flow (2). The physiological response to localized pulmonary hypoxia can cause problems when alveolar hypoxia involves the entire lung. In conditions including chronic obstructive pulmonary disease (3), idiopathic pulmonary fibrosis (4), and at high altitude (5), HPV leads to persistent increases in pulmonary arterial pressures. This in turn causes reduced plasticity of the

vascular bed, sustained pulmonary vascular remodelling and, ultimately, debilitating right ventricular hypertrophy and failure(2).

The hypoxia inducible factors (HIFs) are transcription factors and key regulators of the molecular response to hypoxia. The targets of HIFs include genes controlling vascularization, cellular proliferation, migration, and metabolism(6-11). There have been a number of recent discoveries in human genetics that have correlated HIF function with HPV. For example, individuals with Chuvash polycythemia, a condition with augmented HIF stability under normal oxygen conditions, exhibit enhanced HPV(12). Other mutations resulting in increased expression of the HIF genes have been shown to augment HPV response (13).

A well-characterized animal model of hypoxia-induced pulmonary hypertension involves exposure to chronic hypoxia (CH), typically 10-12% inspired oxygen. This results in extensive vascular remodelling, marked pulmonary hypertension and right ventricular hypertrophy over a period of a few weeks. Exposure to CH in rodents results in vasoconstriction and a pattern of vascular remodelling that is reminiscent of humans with hypoxia-associated pulmonary hypertension (14, 15).

Mice that are hemizygous for either of the HIF isoforms, HIF-1α (16) or HIF-2α (17), have been shown to have attenuated pulmonary vascular remodelling following experimental CH. Conditional deletion of HIF-1α in smooth muscle also ameliorates the degree of remodelling in CH(18). Conversely, mice

homozygous for the R200W mutation that causes Chuvash polycythemia, which acts in part to stabilize HIF-2α, spontaneously develop pulmonary hypertension(19).

HIF-2α is known to modulate the expression of the metalloenzyme arginases (Arg1 and Arg2)(20, 21); both of these arginase isoforms play an important role in the regulation of L-arginine homeostasis and the production of L-ornithine for subsequent polyamine and proline synthesis. These latter are key substrates required for endothelial and smooth muscle cell proliferation and collagen synthesis (22). These isoforms are expressed in vascular endothelial cells and are known to be critical regulators of L-arginine availability and nitric oxide (NO) production via nitric oxide synthases (NOS) (23). NO plays a significant role in the pathogenesis of pulmonary arterial hypertension (PAH), with previous studies identifying lower plasma and exhaled NO in PAH patients than those found in healthy controls (24). Oral supplementation of L-arginine has been suggested to improve hemodynamics and exercise capacity in patients with PAH (25). We have previously demonstrated the roles HIF-1α and HIF-2α play in modulating the expression of NOS2 and Arg-1/-2 in different vascular beds (20, 26), and how this in turn can allow the differential action of the HIF transcription factors to regulate NO homeostasis (21). Under physiological conditions there is sufficient L-arginine available in endothelial cells to convert to NO and L-citrulline. However, prolonged exposure to hypoxia increases the expression of the Arg-1/-2 enzymes, resulting in decreased availability of L-arginine and thus, impaired NO production (27). Conversely, inhibition of arginase activity redirects L-

arginine back towards NOS, allows increased generation of NO, which can in turn alleviate pulmonary hypertension(28).

The mechanisms by which HIF acts in pulmonary vascular remodelling are not fully defined; in particular, the role played by the endothelium in this process is not well understood. Here, we delete the HIF isoforms and one of their targets, the Arg1 gene, specifically in the pulmonary endothelium (29), and show that expression of the HIFα transcription factors in pulmonary endothelial cells is an essential aspect of the hypoxic response of the lung, with broad influence over the development of pulmonary hypertension.

Results

Deletion of HIFα isoforms in pulmonary endothelium

Genetically manipulated mouse strains with conditional alleles of either the HIF-1α or -2α isoforms (30, 31) were crossed to mouse strains expressing the cre recombinase enzyme under the control of the Alk1- or L1 promoter (L1cre) (29). To determine the pulmonary endothelial specificity of this transgene, we analysed the cre activity of adult L1cre mice by crossing with a ROSA26Sor$^{tm9(CAG\text{-}tdTomato)}$ reporter strain. Red fluorescent protein (tdTomato) is expressed following Cre-mediated recombination in this strain background (Supplementary Figure 1A). As shown in supplemental data, lung vasculature in frozen sections was easily identifiable and strongly fluorescent. Minimal expression of tdTomato was detectable in the endothelium of other tissues including heart, spleen and kidney (Supplemental Figure 1B). This is consistent with the published specificity of this transgene (29). Deletion

efficiency was assessed in purified lung endothelial cells by quantitative PCR (qPCR) and deletion frequency was greater than 80% (Supplemental Figure 1C), with little or no detectable deletion in other tissues examined.

HIF-2α deletion in the pulmonary endothelium prevents hypoxia-induced pulmonary hypertension

As an initial test of the importance of endothelial HIF-α stabilisation to the progression of hypoxia induced-pulmonary hypertension, we exposed wild type (WT) and pulmonary endothelial HIF-α deleted mice to normoxic or hypoxic (10% O_2) normobaric atmospheres for 21 days. The development of pulmonary hypertension was then assessed through the measurement of right ventricular systolic pressures (RVSPs), via catheterisation through the jugular vein. Right ventricular systolic pressures in L1cre-HIF-2α mice (18.9±1.0 mmHg, n=11) under normoxic conditions were significantly lower than littermate controls (22.4±1.1 mmHg, n=9, p=0.03) mice. However RVSP from normoxic L1cre-HIF-1α mice (24.7±1.7 mmHg, n=6) did not differ from WT controls (Figure 1A). The rise in RVSP normally observed following chronic hypoxic challenge was essentially absent in mice with pulmonary endothelial HIF-2α deletion. The RVSPs of L1cre-HIF-2α mice following hypoxic exposure (26.1±1.6 mmHg, n=7) were not significantly different from those of untreated WT mice (22.48±1.19, n=9) and were much lower than the elevated values seen in WT littermate controls (41.9±1.8 mmHg, n=12, p<0.0001) and L1cre-HIF-1α mice (36.25±2.37mmHg, n=7, p<0.005).

The ratio of right ventricular weights to those of the left ventricle plus septum (RV/LS+S), an indicator of right ventricular hypertrophy, was likewise

significantly higher in wild-type (0.316±0.01, n=8, p<0.0001) and L1cre-HIF-1α (0.323±0.02, n=8, p<0.001) mice exposed to hypoxia, when compared to the ratios found in L1cre-HIF-2α (0.209±0.008, n=8) mice (Figure 1B). Both red cell counts and hemoglobin values increased while white cell counts decreased following exposure to chronic hypoxia (Supplemental Figure 2A and B). Body weights of all sub-groups, although somewhat variable, trended towards a decrease following exposure to hypoxia (supplemental figure 2C).

Pulmonary endothelial HIF-2α is essential for vascular remodelling

Having established that pulmonary endothelial cell-specific deletion of HIF-2α protects mice from increasing pulmonary pressures in response to chronic hypoxia, we next sought to determine how loss of pulmonary endothelial HIF-2α affects hypoxia-induced vascular remodelling. Serial lung sections were immunostained for smooth muscle actin (α-SMA), in order to detect changes in smooth muscle coverage of the vasculature, and von Willebrand's Factor (vWF) to mark the endothelial cells themselves. The lungs from both wild-type and L1cre-HIF-1α mice demonstrated the typical tissue remodelling seen following chronic hypoxic challenge (Figure 2A). As expected, there was an increase in α-SMA associated with pulmonary arteries that are in close proximity to terminal and respiratory bronchioles (Figure 2A).

However, little to no remodelling was observed in lung sections from L1cre-HIF-2α mice (Figure 2A), reflecting the normal RVSPs observed in these animals following exposure to chronic hypoxia. Lung sections were stained with Verhoeff's stain to detect elastin (32) and thus characterize perivascular collagen deposition; this was increased in both WT controls and L1cre-HIF-1α

mice. However, only minimal staining was seen in the L1cre-HIF-2α mice (Figure 2A). Medial thickening of vessels was then calculated, taking the difference in area circumscribed by the external and internal elastic laminae of pulmonary vessels associated with bronchioles. Both WT littermates (17.82±0.99%, n=15) and L1cre-HIF-1α (14.55±0.99%, n=7) mice showed significantly increased medial thickness following hypoxic conditioning (Figure 2B). In comparison, the L1cre-HIF-2α (10.72±0.74%, n=7) mice showed little change in medial thickness relative to normoxic animals (8.45%±0.69%, n=7) (Supplemental Figure 3).

Another indication of vascular remodelling is the relative amount of collagen deposition in the vasculature. This was significantly higher in hypoxically conditioned WT control and L1cre-HIF-1α mice relative to L1cre-HIF-2α mice (Supplemental Figure 4).

Pulmonary hypertension is also characterised by structural changes to the distal pulmonary vascular bed, including the presence of increased smooth muscle in small peripheral pulmonary arteries. Pulmonary endothelial deletion of HIF-2α reduced smooth muscle cell coverage after hypoxic exposure, with very little α-SMA staining evident in the small peripheral vessels in these animals (Figure 3). In comparison, both WT littermate control and L1cre-HIF-1α mice developed full and partial rings of α-SMA positive cells around vessels in hypoxia-conditioned animals (Figure 3).

Reduced Arginase expression in HIF2α mutant mice

Previous work from our laboratory and others has demonstrated that the two HIFα isoforms act to control NO homeostasis during hypoxia. This occurs at

least in part through HIF1α regulation of the NOS2/iNOS gene, and HIF-2α regulation of the Arg-1 and Arg-2 genes (20, 21, 26, 33, 34). The enzyme Arg-2 in particular has been implicated in reducing airway NO and promoting remodelling and collagen deposition in PAH patients (35, 36). We found that the hypoxia up-regulation of both arg-1 and -2 was completely lost in hypoxia-conditioned isolated pulmonary endothelial cells (Supplemental Figure 5A) and whole lung samples from L1cre-HIF-2α mice relative to WT littermate controls (Figure 4A).

Consistent with these data, we found that plasma $NO_{(X)}$ concentrations were significantly reduced in HIF-1α mice and elevated in the HIF-2α mutant mice compared to WT control mice (Figure 4B); these observations fit a model whereby reduced arginase expression leads to increased availability of L-arginine, and increased NO from NO synthase.

Several recent studies have highlighted the role of endothelin-1(ET-1) in pulmonary hypertension, with elevated expression of this vasoactive agent in a number of patients. The promoter of ET-1 contains HIF transcription factor binding sites, hypoxia response elements (HRE); these sites bind both HIF-1α and HIF-2α (37, 38). However, initial investigations in purified lung endothelial cells from wild-type and L1cre-HIF-2α mice showed little change in ET-1 expression after 24 hours exposure to hypoxia (Supplemental Figure 5B). Furthermore, the gene expression of ET-1 in the lungs of L1cre-HIF-1α and L1cre-HIF-2α mice was did not differ from levels seen in wild type controls following chronic hypoxic challenge (21 days at 10% O_2) (Supplemental Figure 5C). There was a trend towards a decrease in plasma ET-1 in both L1cre-HIF1α and L1cre-HIF2α mice following acute hypoxia, and

a statistically significant decrease in plasma ET-1 in L1cre-HIF2α mice following chronic hypoxia, when compared to wild type controls (Supplemental Figure 5D)

Pulmonary endothelial arginase-1 deletion attenuates PAH

Having established that pulmonary endothelial expression of Arg-1 is significantly reduced in the L1creHIF-2α mouse following chronic hypoxic exposure, we next sought to determine how the specific deletion of arginase-1 in the pulmonary endothelium influenced the development of PAH. The increase in RVSP normally observed following chronic hypoxic challenge (wt, 41.7±0.8mm/Hg, n=7, $p<0.0001$) was significantly attenuated in mice with pulmonary endothelial arginase-1 deletion (31.2±1.0mmHg, n=7) (Figure 5A). Of note, the basal RVSP in L1cre-arg1 mice under normoxia (23.0±0.7mmHg, n=6) were similar to those seen in littermate WT control mice (24.3±0.3mmHg, n=5). The ratio of right ventricular weight to left ventricle plus septum (RV/LS+S) was significantly higher in wild-type (0.39±0.01, n=6, $p<0.001$) when compared to L1cre-arg1 (0.33±0.01, n=9) mice, following chronic hypoxic exposure (Figure 5B). Both red cell counts and hemoglobin scores increased to a similar degree following hypoxic exposure (Supplemental Figure 6A). Wild type littermates showed significantly greater medial thickening (18.57%, n=15) when compared to L1cre-arg1 mice (14.35%, n=9) after exposure to chronic hypoxia (Figure 5C). Similarly, the L1cre-arg1 mice showed substantially less α-SMA associated with pulmonary arteries in close proximity to terminal bronchioles when compared to wild type controls (Supplemental Figure 6B). Staining for α-SMA was also substantially reduced

in the peripheral pulmonary vasculature of these mutants (Figure 5D). Given the importance of Arginase as a regulator of L-arginine availability and NOS-mediated NO production, plasma $NO_{(x)}$ levels were analysed, as described above. Deletion of pulmonary endothelial arg-1 significantly elevated plasma $NO_{(x)}$ relative to the levels seen in plasma from wild type control mice (Figure 5E)

Discussion

The distribution of blood flow through all vascular beds is regulated through constant adjustments to vascular tone. In the lung, these changes preferentially restrict blood flow to areas low in oxygen (2), in contrast to most systemic capillary networks, which react to hypoxia by increasing vasodilation(39, 40). This response by the pulmonary vasculature is complex, involving virtually all cell types of the lung, and can drastically alter lung vascular morphology over time. Remodelling of the pulmonary vasculature is the primary issue in pulmonary hypertension, leading as it does to decreased cardiac and pulmonary function. In this study, we have shown that the endothelial cell specifically is a necessary element in these changes, and that the HIF isoform HIF-2α is in turn required for that endothelial response in hypoxia-induced PH. We also observed the down-regulated expression of arginase in isolated pulmonary endothelial cells and whole lungs from L1cre-HIF2a mice following chronic hypoxia, and demonstrate here that deletion of arginase-1 specifically in the pulmonary endothelium attenuated the development of hypoxic pulmonary hypertension. Given the role of HIF-2α in

regulating arginases specifically, this indicates that a key aspect of the function of HIF-2α in PAH is its regulation of arginase expression.

The pulmonary vascular response to acute hypoxia was first described by von Euler and Liljestrand approximately 75 years ago, and although the physiological consequences are well understood, the molecular regulation of the response, including its cellular components, is less clear (41). The HIF pathway has been implicated in this process for some time, initially through demonstrations showing that mice hemizygous for HIF-1α or HIF-2α have diminished levels of pulmonary hypertension (17, 42). These studies demonstrated the importance of the HIF pathway in the etiology of PAH, and subsequent work was able to show that hemizygosity for HIF-1α resulted in changes in myocyte hypertrophy and polarization (16). In contrast, hemizygosity of HIF-2α revealed that endothelial changes resulting in PAH were partially blocked when HIF-2α was diminished.(17)

More recent work has revealed that tissue-specific loss of HIF-1α in vascular smooth muscle results in some attenuation of hypoxia-induced pulmonary hypertension, but had no effect on a number of other pathologies associated with this syndrome; for example, this deletion had no effect on cardiac remodelling.(18)

These data indicate that both HIF isoforms might play a role in the pathogenesis of hypoxia-induced PAH, however the individual roles of the two major isoforms of HIF, HIF-1α and HIF-2α, and the principal cell types

involved was still uncertain. To address these questions we utilized a cre-recombinase transgene whose expression is restricted to the cells of the pulmonary endothelium (29). As described above, we found that in the pulmonary endothelium, HIF-2α, but not HIF-1α, plays a fundamental role in the development of PAH. Loss of HIF-2α essentially eliminated both pulmonary vascular remodelling and the cardiovascular effects of chronic hypoxic exposure.

Chronic environmental hypoxia results in pulmonary vascular remodelling, which elevates pulmonary vascular resistance, and leads to right ventricular pressure overload (43). Structural changes include the appearance of smooth muscle-like cells in small pulmonary arterioles and medial and adventitial thickening of muscular and elastic vessels (44). In this study, hypoxia failed to induce smooth muscle accumulation in the pre-capillary vessels in HIF-2α pulmonary endothelial mutant animals, and the medial thickening of vessels associated with terminal bronchi was also substantially reduced. These data are quite similar qualitatively to the effects seen in hemizygous HIF-2α mice, pointing to the pulmonary endothelium as the dominant cell type in mediating the effect of HIF-2α during pulmonary hypertensive remodelling.

Collagen accumulation contributes to pulmonary artery stiffening in hypoxic induced pulmonary hypertension. In clinical studies an increase in pulmonary artery stiffness has been found to be a strong predictor of mortality in patients with PAH (45). In this report, prolonged exposure of wild-type and L1cre-HIF-1α mice to hypoxia resulted in a significant accumulation of collagen around bronchial associated arteries; in comparison, deletion of pulmonary

endothelial HIF-2α significantly reduced collagen accumulation, likely contributing to the lower RVSP seen in these animals.

Hypoxic modulation of endothelin-1 has been suggested by several studies as a potential mechanism driving hypoxic pulmonary vasoconstriction (17, 46, 47). Although we cannot discount a role for pulmonary endothelial derived ET-1 in the development of PAH, we observed similar acute hypoxic changes in plasma ET-1 expression following deletion of either of the HIF-α isoforms. Further investigations are clearly required to clarify the link between endothelin-1, HIFα expression, and PAH.

The causal link between pulmonary hypertension and NO homeostasis has been extensively documented (35, 48), and this is reflected clinically in the finding that intrapulmonary nitrates, biochemical reaction products of NO in bronchoalveolar fluid, and exhaled NO are all diminished in human pulmonary hypertension (24, 49). Interestingly, primary pulmonary endothelial cells isolated from PAH patients have substantially increased expression of arg-2 (36), which would be predicted to decrease available L-arginine and reduce NOS-derived NO formation. We have previously shown that both Arg1 and Arg2 are HIF-2α-dependent genes, and we show here that their expression in pulmonary endothelium is decreased in HIF-2α pulmonary endothelium mutants. This should result in an increase in pulmonary endothelial NO, which itself has been shown to alleviate PAH experimentally (50). Consistent with this hypothesis, genetic deletion of arg-1 resulted in a marked attenuation in the pathologies associated with PAH. Given a mechanistic link between

these findings and the etiology of PAH, future therapies to manipulate the control of NO homeostasis by the HIFα pathway should certainly be explored.

Pulmonary hypertension due to chronic hypoxia is a progressive disease, that leads eventually to right heart failure and death. The pathogenesis of this condition involves proliferation of endothelial and smooth muscle cells, resulting in vascular remodeling of the pulmonary arterioles. Here we identify an essential role for pulmonary endothelial HIF2α expression, and its regulation of arginase, in both the physiological response to acute hypoxia, and the vascular remodelling processes that characterise chronic hypoxic exposure.

Methods

Animals. All animals were housed in an Association and Accreditation of Laboratory Animal Care International-approved facility. All protocols and surgical procedures were approved by the local and national animal care committees.

Targeted deletion of HIF-1α, HIF-2α and arginase-1 in pulmonary endothelial cells was created by crossing (C57Bl6/j) homozygous for the floxed allele in HIF-1α, HIF-2α or arginase-1 into a background of Cre recombinase expression drive by the L1 (alk-1) promoter kindly donate by Dr Paul Oh, Florida University.(29) Mice characterized as wild type (WT) were in all cases littermates of respective mutant mice, homozygous for conditional alleles but without the cre recombinase transgene.

Measurement of Right Ventricular Systolic Pressure (RVSP). For induction of PAH due to chronic hypoxia, groups of male mice (8-12 weeks) were maintained in a normobaric hypoxic chamber (FiO_2 10%) for up to 21 days. Mice were weighed then anesthetised (isoflurane) and right-sided heart catheterisation through the right jugular using a pressure-volume loop catheter (Millar).(51-53) Bloods were taken for haemodynamic assessment.

Right Ventricular Hypertrophy. To measure the extent of right ventricular hypertrophy (RVH), the heart was removed and the right ventricule (RV) free wall was dissected from the left ventricle plus septum (LV+S), and weighed separately.(54) The degree of RVH was determined from the ratio RV/LV+S.

Tissue Preparation. In all animals the left lung was fixed *in situ* in the distended state by the infusion of 0.8% agarose into the trachea, and then placed in 10% paraformaldehyde before paraffin embedding. The right lung was frozen in liquid nitrogen for mRNA extraction.

Pulmonary Vascular Morphometry. Lung tissues were stained with hematoxylin and eosin, sirius red or elastic van Gieson (EVG) stain to assess morphology (all Merck/BDH, Lutterworth UK). To determine the degree of muscularization of small pulmonary arteries, serial lung tissue sections were stained with anti-smooth muscle α-actin (α-SMactin; DakoCytomation Ely UK) and von Willebrand factor (DakoCytomation). Antibody staining was visualised using 3-3' diaminobenzidine hydrochloride substrate (DakoCytomation) and counterstained with Carrazzi hematoxylin (Bios Shelmersdale UK). Vessel medial thickness was measured using Image J software (MediaCybernetics, Bethesda MD)

Haematological Analysis. Anti-coagulated blood was analysed using Vet abc haematology analyser (Horiba) according to the manufacturers instructions.

Nitrite/Nitrate Analysis. Blood samples were centrifuged to separate plasma and were passed through a column with a 10-kDa cut-off filter. All samples were analysed for total $NO_{(X)}$ content using a NOA 280i (Siever, GE Healthcare) according to the manufacturers instructions.

RNA Analysis. Total RNA and DNA was isolated from the lung using TRI-reagent (Sigma) followed by RNA clean-up and DNase digest using RNeasy column kits (Qiagen). First-strand synthesis was performed with 1μg of total RNA using a high-capacity cDNA kit (Applied Biosystems) according to the manufacturers instructions. Relative gene expression was determined by quantitative PCR (qPCR) (One-Step Plus Real-Time PCR System; Life Technologies) and was amplified in SYBR-Green master mix (Roche) and relevant primers from Qiagen. Relative gene-expression levels were related to β-actin and B_2M using the $2\Delta\Delta CT$ method.

Statistical Analysis. All data represents the mean (±SEM) of *n* separate experiments unless otherwise stated. Difference between groups were assessed using *t* test unless otherwise stated. A *p* value of <0.05 was considered significant.

Acknowledgement. We thank Dr Paul Oh from Department of Physiology and Functional Genomics, University of Florida for kindly allow us to use the L1(alk-1)cre mouse.

Funding Sources

This study was funded by The Wellcome Trust, Papworth Hospital NIHR Cambridge Biomedical Research Centre.

Disclosures

None.

References

1. von Euler US, Liljestrand, G. (1946) Observations on the pulmonary arterial blood pressure in the cat. *Acta Physiologica Scand* 12:19.
2. Sylvester JT, Shimoda LA, Aaronson PI, & Ward JP (2012) Hypoxic pulmonary vasoconstriction. *Physiol Rev* 92(1):367-520.
3. Naeije R (2005) Pulmonary hypertension and right heart failure in chronic obstructive pulmonary disease. *Proc Am Thorac Soc* 2(1):20-22.
4. Lettieri CJ, Nathan SD, Barnett SD, Ahmad S, & Shorr AF (2006) Prevalence and outcomes of pulmonary arterial hypertension in advanced idiopathic pulmonary fibrosis. *Chest* 129(3):746-752.
5. Bartsch P & Gibbs JS (2007) Effect of altitude on the heart and the lungs. *Circulation* 116(19):2191-2202.
6. Semenza GL (2003) Targeting HIF-1 for cancer therapy. *Nature reviews. Cancer* 3(10):721-732.
7. Semenza GL (2009) Regulation of vascularization by hypoxia-inducible factor 1. *Ann N Y Acad Sci* 1177:2-8.
8. Pouyssegur J, Dayan F, & Mazure NM (2006) Hypoxia signalling in cancer and approaches to enforce tumour regression. *Nature* 441(7092):437-443.
9. Formenti F*, et al.* (2010) Regulation of human metabolism by hypoxia-inducible factor. *Proceedings of the National Academy of Sciences of the United States of America* 107(28):12722-12727.
10. Djagaeva I & Doronkin S (2010) Hypoxia response pathway in border cell migration. *Cell Adh Migr* 4(3):391-395.
11. Hubbi ME*, et al.* (2014) Cyclin-dependent kinases regulate lysosomal degradation of hypoxia-inducible factor 1alpha to promote cell-cycle progression. *Proceedings of the National Academy of Sciences of the United States of America* 111(32):E3325-3334.
12. Smith TG*, et al.* (2006) Mutation of von Hippel-Lindau tumour suppressor and human cardiopulmonary physiology. *PLoS Med* 3(7):e290.
13. Formenti F*, et al.* (2011) Cardiopulmonary function in two human disorders of the hypoxia-inducible factor (HIF) pathway: von Hippel-Lindau disease and HIF-2alpha gain-of-function mutation. *FASEB journal : official publication of the Federation of American Societies for Experimental Biology* 25(6):2001-2011.
14. Stenmark KR, Meyrick B, Galie N, Mooi WJ, & McMurtry IF (2009) Animal models of pulmonary arterial hypertension: the hope for etiological discovery and pharmacological cure. *American journal of physiology. Lung cellular and molecular physiology* 297(6):L1013-1032.
15. Dickinson MG, Bartelds B, Borgdorff MA, & Berger RM (2013) The role of disturbed blood flow in the development of pulmonary arterial hypertension: lessons from preclinical animal models. *American journal of physiology. Lung cellular and molecular physiology* 305(1):L1-14.
16. Shimoda LA, Manalo DJ, Sham JS, Semenza GL, & Sylvester JT (2001) Partial HIF-1alpha deficiency impairs pulmonary arterial myocyte electrophysiological responses to hypoxia. *American journal of physiology. Lung cellular and molecular physiology* 281(1):L202-208.

17. Brusselmans K*, et al.* (2003) Heterozygous deficiency of hypoxia-inducible factor-2alpha protects mice against pulmonary hypertension and right ventricular dysfunction during prolonged hypoxia. *The Journal of clinical investigation* 111(10):1519-1527.
18. Ball MK*, et al.* (2014) Regulation of hypoxia-induced pulmonary hypertension by vascular smooth muscle hypoxia-inducible factor-1alpha. *American journal of respiratory and critical care medicine* 189(3):314-324.
19. Hickey MM, Lam JC, Bezman NA, Rathmell WK, & Simon MC (2007) von Hippel-Lindau mutation in mice recapitulates Chuvash polycythemia via hypoxia-inducible factor-2alpha signaling and splenic erythropoiesis. *The Journal of clinical investigation* 117(12):3879-3889.
20. Cowburn AS*, et al.* (2013) HIF isoforms in the skin differentially regulate systemic arterial pressure. *Proceedings of the National Academy of Sciences of the United States of America* 110(43):17570-17575.
21. Takeda N*, et al.* (2010) Differential activation and antagonistic function of HIF-{alpha} isoforms in macrophages are essential for NO homeostasis. *Genes & development* 24(5):491-501.
22. Li H*, et al.* (2001) Regulatory role of arginase I and II in nitric oxide, polyamine, and proline syntheses in endothelial cells. *Am J Physiol Endocrinol Metab* 280(1):E75-82.
23. Krotova K, Patel JM, Block ER, & Zharikov S (2010) Hypoxic upregulation of arginase II in human lung endothelial cells. *Am J Physiol Cell Physiol* 299(6):C1541-1548.
24. Kaneko FT*, et al.* (1998) Biochemical reaction products of nitric oxide as quantitative markers of primary pulmonary hypertension. *American journal of respiratory and critical care medicine* 158(3):917-923.
25. Nagaya N*, et al.* (2001) Short-term oral administration of L-arginine improves hemodynamics and exercise capacity in patients with precapillary pulmonary hypertension. *American journal of respiratory and critical care medicine* 163(4):887-891.
26. Branco-Price C*, et al.* (2012) Endothelial cell HIF-1alpha and HIF-2alpha differentially regulate metastatic success. *Cancer cell* 21(1):52-65.
27. Berkowitz DE*, et al.* (2003) Arginase reciprocally regulates nitric oxide synthase activity and contributes to endothelial dysfunction in aging blood vessels. *Circulation* 108(16):2000-2006.
28. Chu Y*, et al.* (2016) Arginase inhibitor attenuates pulmonary artery hypertension induced by hypoxia. *Mol Cell Biochem* 412(1-2):91-99.
29. Park SO*, et al.* (2008) ALK5- and TGFBR2-independent role of ALK1 in the pathogenesis of hereditary hemorrhagic telangiectasia type 2. *Blood* 111(2):633-642.
30. Ryan HE*, et al.* (2000) Hypoxia-inducible factor-1alpha is a positive factor in solid tumor growth. *Cancer research* 60(15):4010-4015.
31. Gruber M*, et al.* (2007) Acute postnatal ablation of Hif-2alpha results in anemia. *Proceedings of the National Academy of Sciences of the United States of America* 104(7):2301-2306.

32. Yamataka T & Puri P (1997) Pulmonary artery structural changes in pulmonary hypertension complicating congenital diaphragmatic hernia. *J Pediatr Surg* 32(3):387-390.
33. Melillo G*, et al.* (1995) A hypoxia-responsive element mediates a novel pathway of activation of the inducible nitric oxide synthase promoter. *J Exp Med* 182(6):1683-1693.
34. Louis CA*, et al.* (1998) Distinct arginase isoforms expressed in primary and transformed macrophages: regulation by oxygen tension. *The American journal of physiology* 274(3 Pt 2):R775-782.
35. Grasemann H*, et al.* (2015) Arginase inhibition prevents bleomycin-induced pulmonary hypertension, vascular remodeling, and collagen deposition in neonatal rat lungs. *American journal of physiology. Lung cellular and molecular physiology* 308(6):L503-510.
36. Xu W*, et al.* (2004) Increased arginase II and decreased NO synthesis in endothelial cells of patients with pulmonary arterial hypertension. *FASEB journal : official publication of the Federation of American Societies for Experimental Biology* 18(14):1746-1748.
37. Yamashita K, Discher DJ, Hu J, Bishopric NH, & Webster KA (2001) Molecular regulation of the endothelin-1 gene by hypoxia. Contributions of hypoxia-inducible factor-1, activator protein-1, GATA-2, AND p300/CBP. *The Journal of biological chemistry* 276(16):12645-12653.
38. Camenisch G, Stroka DM, Gassmann M, & Wenger RH (2001) Attenuation of HIF-1 DNA-binding activity limits hypoxia-inducible endothelin-1 expression. *Pflugers Arch* 443(2):240-249.
39. Kuwahira I, Gonzalez NC, Heisler N, & Piiper J (1993) Changes in regional blood flow distribution and oxygen supply during hypoxia in conscious rats. *Journal of applied physiology* 74(1):211-214.
40. Talks KL*, et al.* (2000) The expression and distribution of the hypoxia-inducible factors HIF-1alpha and HIF-2alpha in normal human tissues, cancers, and tumor-associated macrophages. *The American journal of pathology* 157(2):411-421.
41. Dweik RA*, et al.* (2014) An official American Thoracic Society Statement: pulmonary hypertension phenotypes. *American journal of respiratory and critical care medicine* 189(3):345-355.
42. Yu AY*, et al.* (1999) Impaired physiological responses to chronic hypoxia in mice partially deficient for hypoxia-inducible factor 1alpha. *The Journal of clinical investigation* 103(5):691-696.
43. McLaughlin VV & McGoon MD (2006) Pulmonary arterial hypertension. *Circulation* 114(13):1417-1431.
44. Stenmark KR, Fagan KA, & Frid MG (2006) Hypoxia-induced pulmonary vascular remodeling: cellular and molecular mechanisms. *Circ Res* 99(7):675-691.
45. Wang Z, Lakes RS, Eickhoff JC, & Chesler NC (2013) Effects of collagen deposition on passive and active mechanical properties of large pulmonary arteries in hypoxic pulmonary hypertension. *Biomech Model Mechanobiol* 12(6):1115-1125.
46. Pisarcik S*, et al.* (2013) Activation of hypoxia-inducible factor-1 in pulmonary arterial smooth muscle cells by endothelin-1. *American journal of physiology. Lung cellular and molecular physiology* 304(8):L549-561.

47. Skuli N*, et al.* (2009) Endothelial deletion of hypoxia-inducible factor-2alpha (HIF-2alpha) alters vascular function and tumor angiogenesis. *Blood* 114(2):469-477.
48. Machado RF*, et al.* (2004) Nitric oxide and pulmonary arterial pressures in pulmonary hypertension. *Free radical biology & medicine* 37(7):1010-1017.
49. Girgis RE*, et al.* (2005) Decreased exhaled nitric oxide in pulmonary arterial hypertension: response to bosentan therapy. *American journal of respiratory and critical care medicine* 172(3):352-357.
50. Budts W*, et al.* (2000) Aerosol gene transfer with inducible nitric oxide synthase reduces hypoxic pulmonary hypertension and pulmonary vascular remodeling in rats. *Circulation* 102(23):2880-2885.
51. Crosby A*, et al.* (2011) Praziquantel reverses pulmonary hypertension and vascular remodeling in murine schistosomiasis. *American journal of respiratory and critical care medicine* 184(4):467-473.
52. Crosby A*, et al.* (2010) Pulmonary vascular remodeling correlates with lung eggs and cytokines in murine schistosomiasis. *American journal of respiratory and critical care medicine* 181(3):279-288.
53. Crosby A*, et al.* (2015) Hepatic Shunting of Eggs and Pulmonary Vascular Remodeling in Bmpr2(+/-) Mice with Schistosomiasis. *American journal of respiratory and critical care medicine* 192(11):1355-1365.
54. Morrell NW, Atochina EN, Morris KG, Danilov SM, & Stenmark KR (1995) Angiotensin converting enzyme expression is increased in small pulmonary arteries of rats with hypoxia-induced pulmonary hypertension. *The Journal of clinical investigation* 96(4):1823-1833.

Figure Legends

Figure 1. Pulmonary endothelial HIF-2α modulates chronic hypoxic pulmonary hypertension. (A) Scatter plot (mean ± SEM) shows the effect of pulmonary endothelial HIFα on right ventricular systolic pressure (RVSP). Wild-type (WT) and L1cre-HIFα mice were housed in normoxia (N) or chronic hypoxia (H) (WT (N) n=9 (H) n=12; L1cre-HIF-1α (N) n= 6 (H) n=7; L1cre-HIF-2α (N) n=11 (H) n=7). (B) Effect of pulmonary endothelial HIFα on right ventricular hypertrophy. Scatter plot (mean ± SEM) show RV/LV+S weight ratio in mice exposed to normoxia (N) or chronic hypoxia (H) (WT (N) n=9 (H) n=12; L1cre-HIF-1α (N) n= 6 (H) n=7; L1cre-HIF-2α (N) n=11 (H) n=7). *P<0.05, **P<0.001, ***P<0.0001

Figure 2. Pulmonary endothelial HIF-2α is essential for airway remodelling in chronic hypoxic pulmonary hypertension. (A and B) Airway remodelling was determined in wild-type (WT) (n=15), L1cre-HIF-1α (n=7) and L1cre-HIF-2α (n=7) post chronic hypoxic challenge. (A) Histological sections of lung were immunostained with α–smooth-muscle actin(α-SMA), von Willebrand factor(vWF), and Elastic van Gieson (EVG). Representative photomicrographs demonstrate the remarkable lack of remodelling in L1cre-HIF-2α pulmonary arteries associated with terminal bronchi when compared to WT or L1cre-HIF-1α mice. (B) Scatter plot (mean ± SEM) shows the effect of pulmonary endothelial HIFα on vessel medial thickness. Quantification of the intimal medial thickness achieved by staining lung sections with EVG. Measurement of vessel thickness as a percentage of total vessel area by image J software. ***P<0.0001.

Figure 3. Loss of HIF-2α in pulmonary endothelial cells reduces the degree of muscularization of peripheral arteries. Stacked bar chart showing the degree of muscularization of peripheral pulmonary arteries in lung sections from wild-type (WT) (n=15), L1cre-HIF-1α (n=9) and L1cre-HIF-2α (n=7) mice. Representative photomicrographs immunostained for α-smooth muscle actin showing near and complete ring formation in peripheral vessel of WT and L1cre-HIF-1α mice when compared to L1cre-HIF-2α mice (arrows point to distal vessels).

Figure 4. Endothelial deletion of HIF-2α maintains higher plasma nitrate levels potentially through lower arginase expression in pulmonary endothelium. (A) qPCR analysis of arginase-I/-II, NOS2, and VEGF mRNA from whole lung samples of wild-type (WT) (open bar, n=7), L1cre-HIF-1α (dark grey bar, n=7) and L1cre-HIF-2α (closed bar, n=6). (B) Total nitric oxide was determined in the plasma by the conversion of NO_x to NO using a nitric oxide analyser (Siever). Data shown as scatter plot with mean ± SEM from WT (n=7), L1cre-HIF-1α (n=7) and L1cre-HIF-2α (n=6) post chronic hypoxia challenge. *P<0.05.

Figure 5. Pulmonary endothelial deletion of Arg-1 attenuates hypoxic pulmonary hypertensive phenotype. A) Scatter plot (mean ± SEM) shows the effect of pulmonary endothelial Arg-1 on right ventricular systolic pressure (RVSP). Wild-type (WT) and L1cre-Arg1 mice were housed in normoxia (N) or chronic hypoxia (H) (WT (N) n=5 (H) n=7; L1cre-Arg1 (N) n= 6 (H) n=7. (B)

Effect of pulmonary endothelial Arg-1 on right ventricular hypertrophy. Scatter plot (mean ± SEM) show RV/LV+S weight ratio in mice exposed to normoxia (N) or chronic hypoxia (H) (WT (N) n=6 (H) n=6; L1cre-Arg1 (N) n= 7 (H) n=9. (C) Airway remodelling was determined in wild-type (WT) (n=8), L1cre-Arg1 (n=10). Quantification of the intimal medial thickness achieved by staining lung sections with EVG. Measurement of vessel thickness as a percentage of total vessel area by image J software. (D) Stacked bar chart showing the degree of muscularization of peripheral pulmonary arteries in lung sections from wild-type (WT) (n=5), L1cre-Arg1 (n=6) mice. Representative photomicrographs immunostained for α-smooth muscle actin showing near and complete ring formation in peripheral vessel of WT mice when compared to L1cre-Arg1 mice. (E) Total nitric oxide was determined in the plasma by the conversion of NO_x to NO using a nitric oxide analyser (Siever). Data shown as scatter plot with mean ± SEM from WT (n=6), L1cre-Arg1 (n=8) post chronic hypoxia challenge; *P<0.05, **P<0.001, ***P<0.0001.

Figure 1

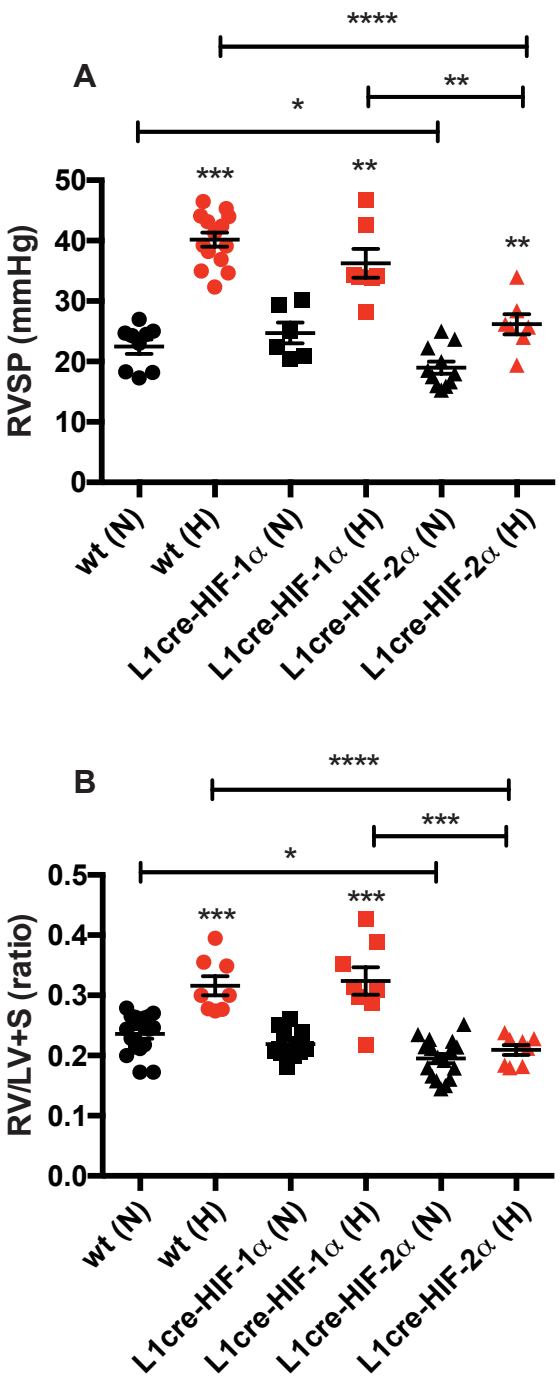
A
****
**
*
***
**
**
RVSP (mmHg)
50
40
30
20
10
0
wt (N)
wt (H)
L1cre-HIF-1α (N)
L1cre-HIF-1α (H)
L1cre-HIF-2α (N)
L1cre-HIF-2α (H)
B
****
***
*
***
***
RV/LV+S (ratio)
0.5
0.4
0.3
0.2
0.1
0.0
wt (N)
wt (H)
L1cre-HIF-1α (N)
L1cre-HIF-1α (H)
L1cre-HIF-2α (N)
L1cre-HIF-2α (H)

Figure 2

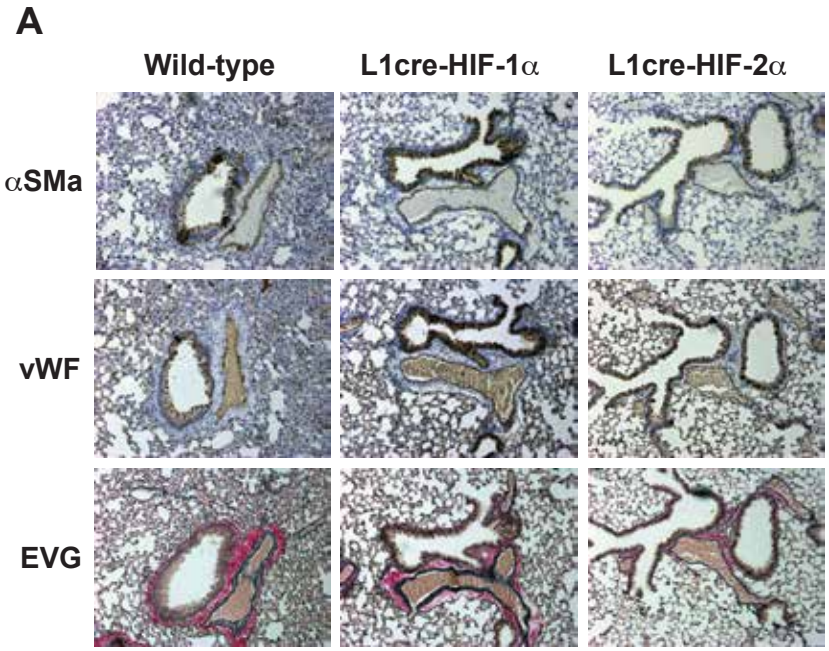
A
Wild-type
L1cre-HIF-1α
L1cre-HIF-2α
αSMa
vWF
EVG

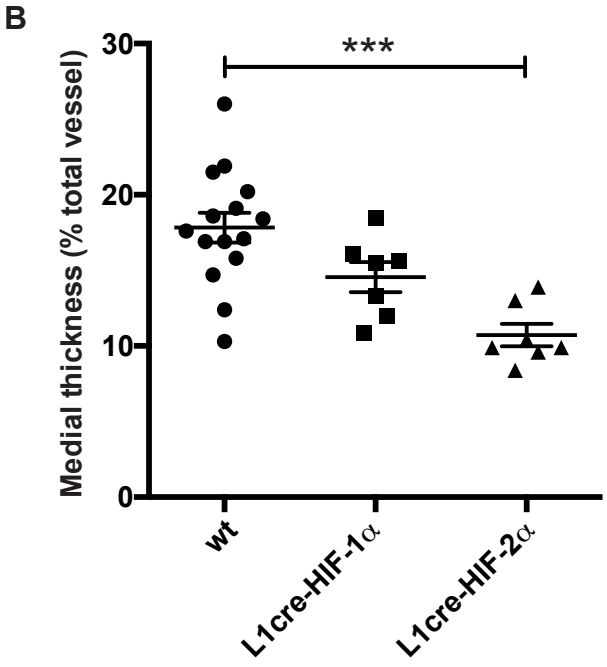
B
***
Medial thickness (% total vessel)
30
20
10
0
wt
L1cre-HIF-1α
L1cre-HIF-2α

Figure 3

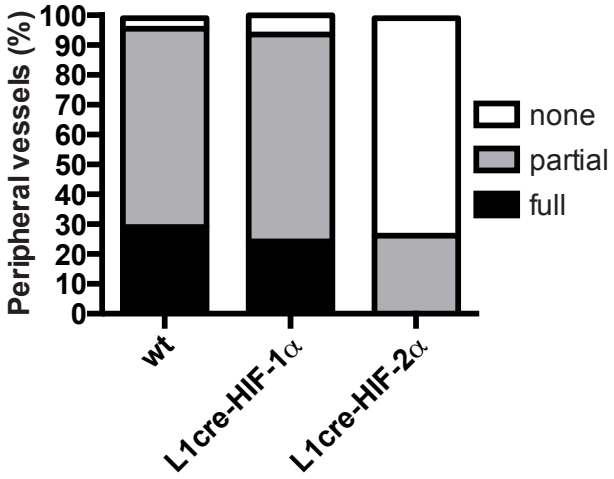
Peripheral vessels (%)
100
90
80
70
60
50
40
30
20
10
0
none
partial
full
wt
L1cre-HIF-1α
L1cre-HIF-2α

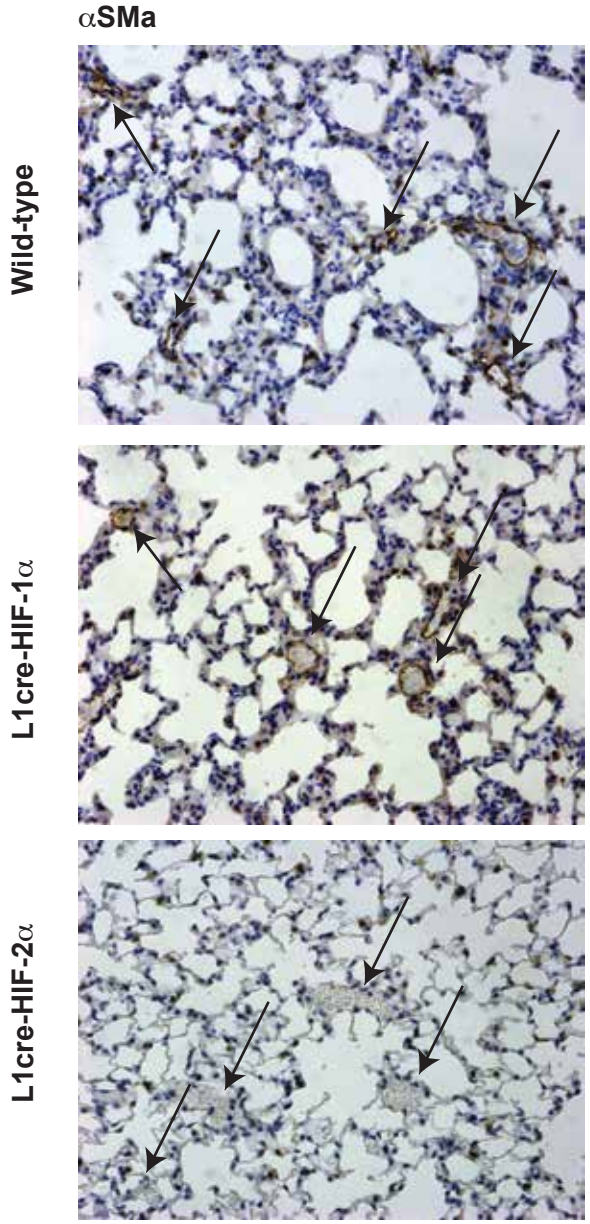
αSMa
Wild-type
L1cre-HIF-1α
L1cre-HIF-2α

Figure 4

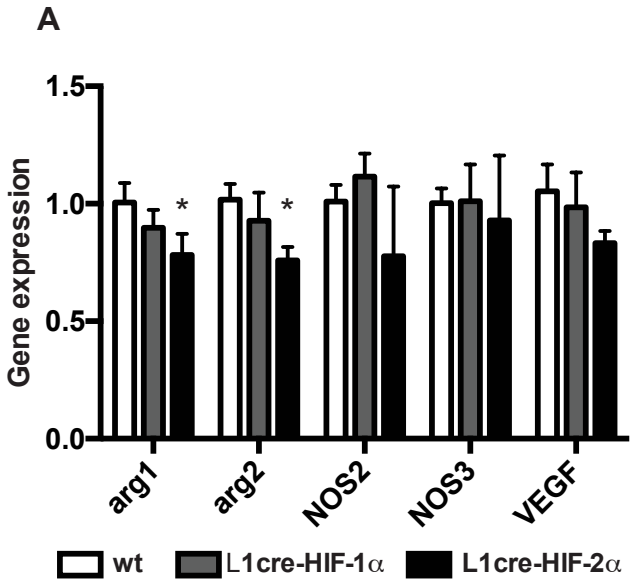
A
1.5
1.0
0.5
0.0
Gene expression
*
*
arg1
arg2
NOS2
NOS3
VEGF
wt
L1cre-HIF-1α
L1cre-HIF-2α

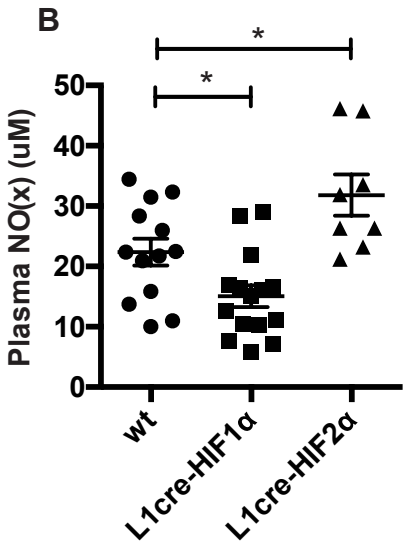
B
*
*
50
40
30
20
10
0
Plasma NO(x) (uM)
wt
L1cre-HIF1α
L1cre-HIF2α

Figure 5

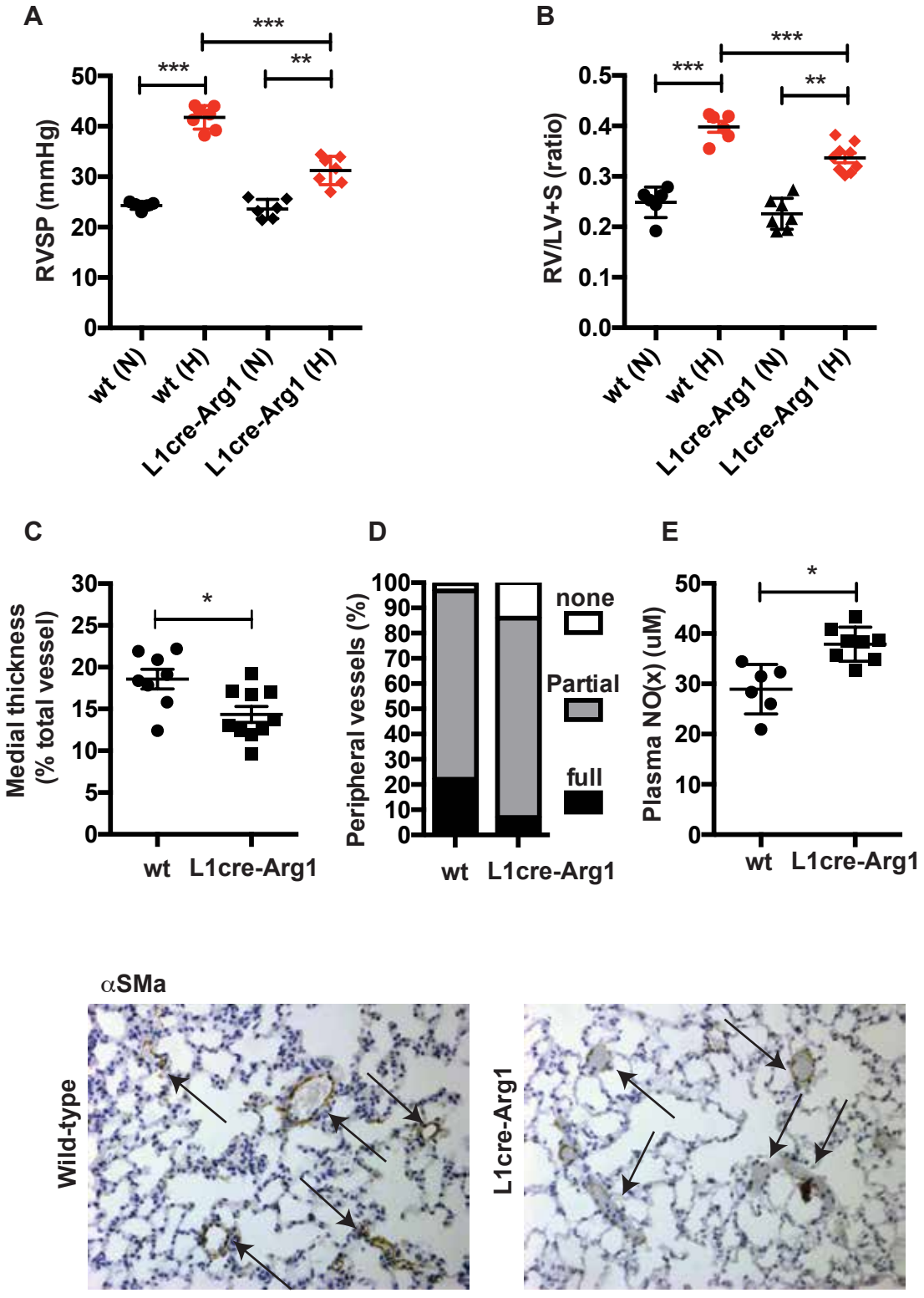
A
RVSP (mmHg)
50
40
30
20
10
0
***
***
**
wt (N)
wt (H)
L1cre-Arg1 (N)
L1cre-Arg1 (H)
B
RV/LV+S (ratio)
0.5
0.4
0.3
0.2
0.1
0.0
***
***
**
wt (N)
wt (H)
L1cre-Arg1 (N)
L1cre-Arg1 (H)
C
Medial thickness (% total vessel)
30
25
20
15
10
5
0
*
wt
L1cre-Arg1
D
Peripheral vessels (%)
100
90
80
70
60
50
40
30
20
10
0
none
Partial
full
wt
L1cre-Arg1
E
Plasma NO(x) (uM)
50
40
30
20
10
0
*
wt
L1cre-Arg1
αSMa
Wild-type
L1cre-Arg1

Supplemental Figures:

Supplemental Figure 1. L1cre specificity for pulmonary endothelial cells. Representative photomicrographs from 3 independent mice (A) show bright-field structure of frozen lung sections, strong positive fluorescent endothelial cells and combined overlay. (B) Frozen tissue sections taken from representative organs in the same L1cre mouse. Little to no positive fluorescent cells were seen in other tissues. (C) L1cre deletion efficiency of HIF-2α in isolated pulmonary endothelial cells and other selected organs. Isolated endothelial data shown as single experiment from six pooled animals.

Supplemental Figure 2. Haematological and body weight response to chronic hypoxia. (A and B) Red blood cell counts (RBC), haemoglobin (HGB) scores and white cell counts (WBC) did not deviate between the groups (A) Data shown as scatter graph as mean ± SEM of RBC and HGB from normoxic (N) and chronic hypoxic (H) housed wild-type (WT) (n=9 and n=15) L1cre-HIF-1α (n=9 and n=8) and L1cre-HIF-2α (n=7 and n=8). (C) Bar graph of mean ± SEM body weight, normoxic (N) and after chronic hypoxia (H) from WT (n=8), L1cre-HIF-1α (n=7) and L1cre-HIF-2α (n=8).

Supplemental Figure 3. Histological sections from paraffin wax embedded lungs were immunostained for αSmooth-Muscle actin, von Willebrand factor, and

stained for hematoxylin & eosin and Elastic van Gieson (EVG). Representative photomicrographs show no remodelling in normoxic housed L1cre-HIF-1α or L1cre-HIF-2α mice when compared to wild-type control.

Supplemental Figure 4. Deletion of pulmonary endothelial HIF-2α decreases collagen deposition around arteries associated with terminal bronchus. Histological lung sections were stained using Sirius red and then analysed by image J software. Data shown as bar graph for wild-type (WT) (open bar, n=7), L1cre-HIF-1α (grey bar, n=6) and L1cre-HIF-2α (closed bar, n=7). Representative photomicrographs show the degree of collagen deposition following chronic hypoxic challenge. **P<0.001

Supplemental Figure 5. Arginase and Endothelin-1 expression in isolated pulmonary endothelial cells and whole lung. (A and B) QPCR data from a single experiment of six pool animals, pulmonary endothelial cells isolated from wild-type or L1cre-HIF-2α mice culture in normoxia or hypoxia for 24hrs. (C) QPCR analysis of ET-1 expression in whole lung tissue from wild-type (n=15), L1cre-HIF-1α (n=7) and L1cre-HIF-2α (n=6) mice following chronic hypoxic challenge. (C) Acute hypoxic increase in plasma endothelin-1 was inhibited in the L1cre-

HIF1a (n=4) and L1cre-HIF2a (n=4) mice when compared to wild-type (n=6). Data bar shown as mean ± SEM

Supplemental Figure 6. Red blood cell counts (RBC), haemoglobin (HGB) did not deviate between the groups (A) Data shown as scatter graph as mean ± SEM of RBC and HGB from normoxic (N) and chronic hypoxic (H) housed wild-type (WT) (n=6(N) and 4(H)) L1cre-Arg1 (n=6 (N) and n=9(H)) (B) Histological sections of lung were immunostained with α–smooth-muscle actin(α-SMA), von Willebrand factor(vWF), and Elastic van Gieson (EVG). Representative photomicrographs demonstrate the attenuation of remodelling in L1cre-Arg1 pulmonary arteries associated with terminal bronchi when compared to WT controls.

Supplemental Figure 1

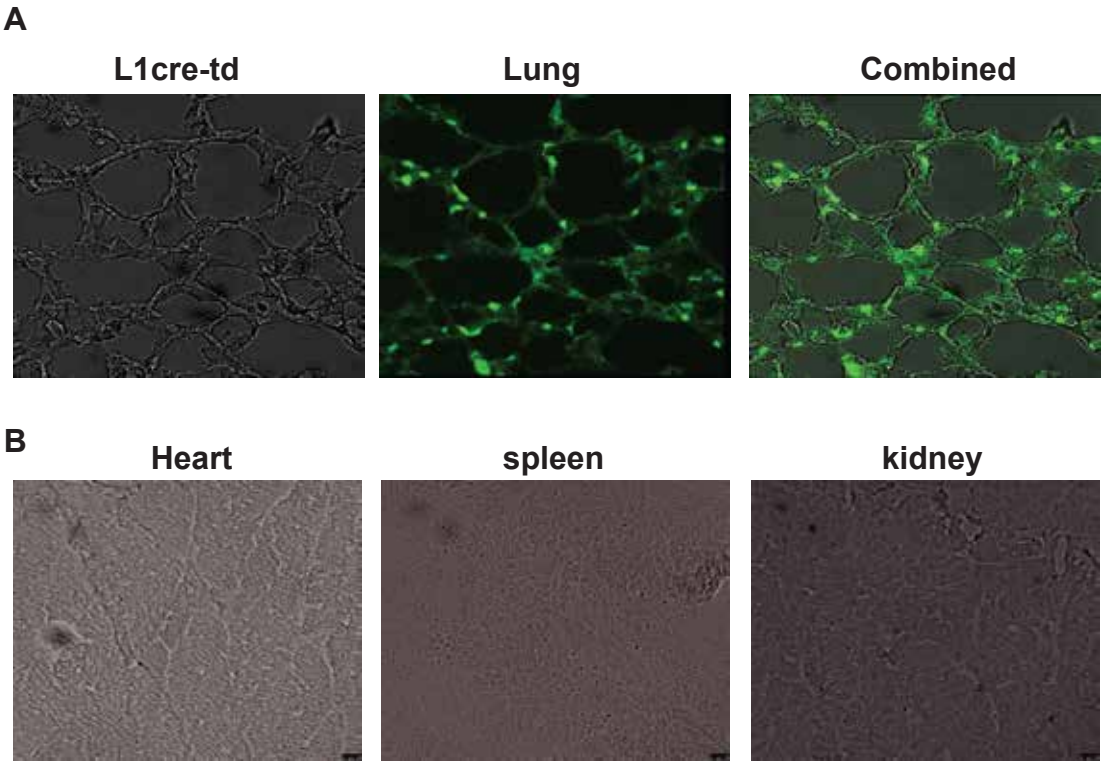

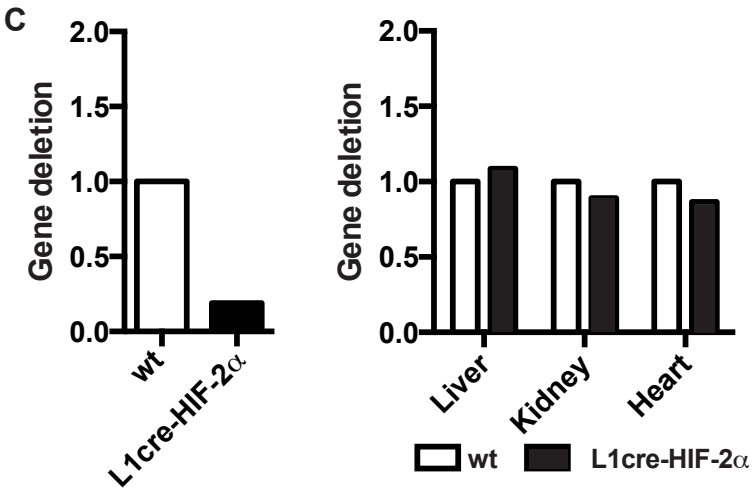

Supplemental Figure 2

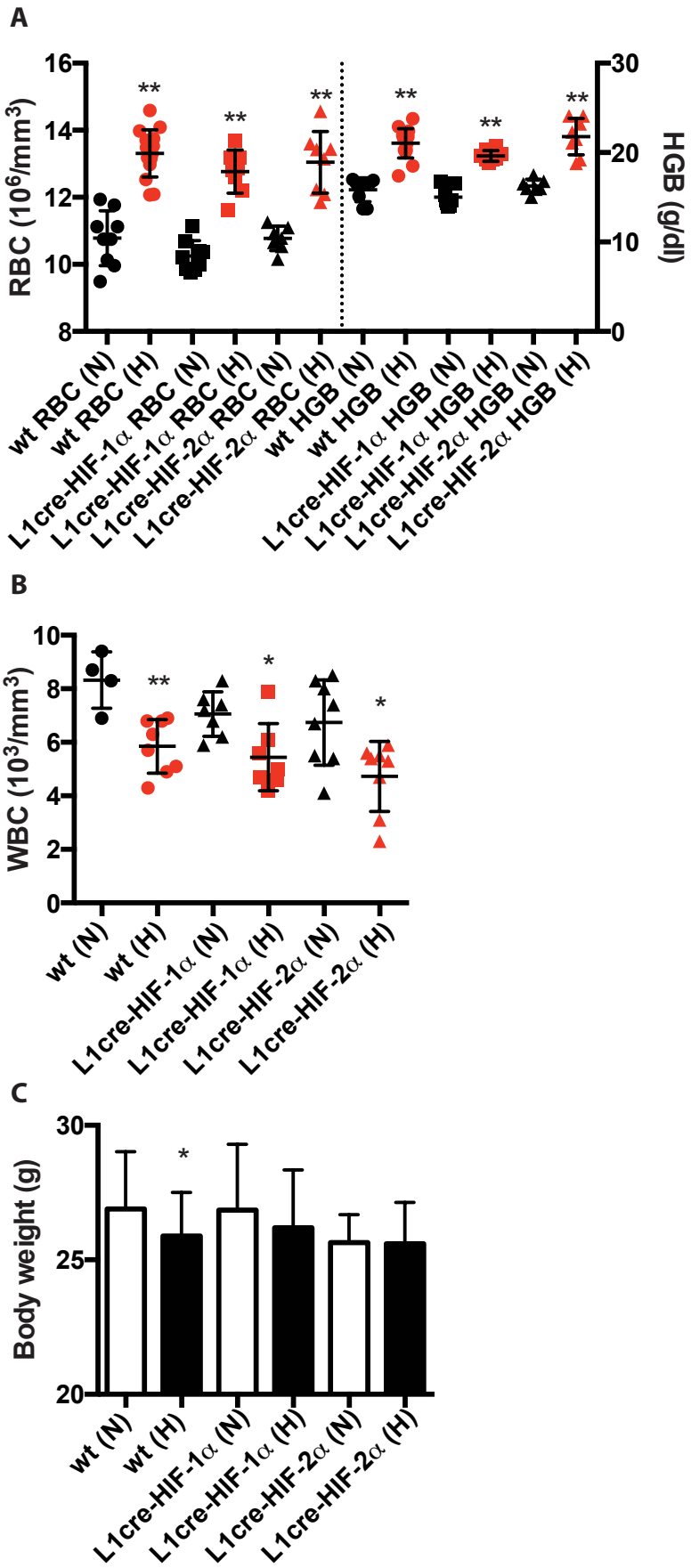

Supplemental Figure 3

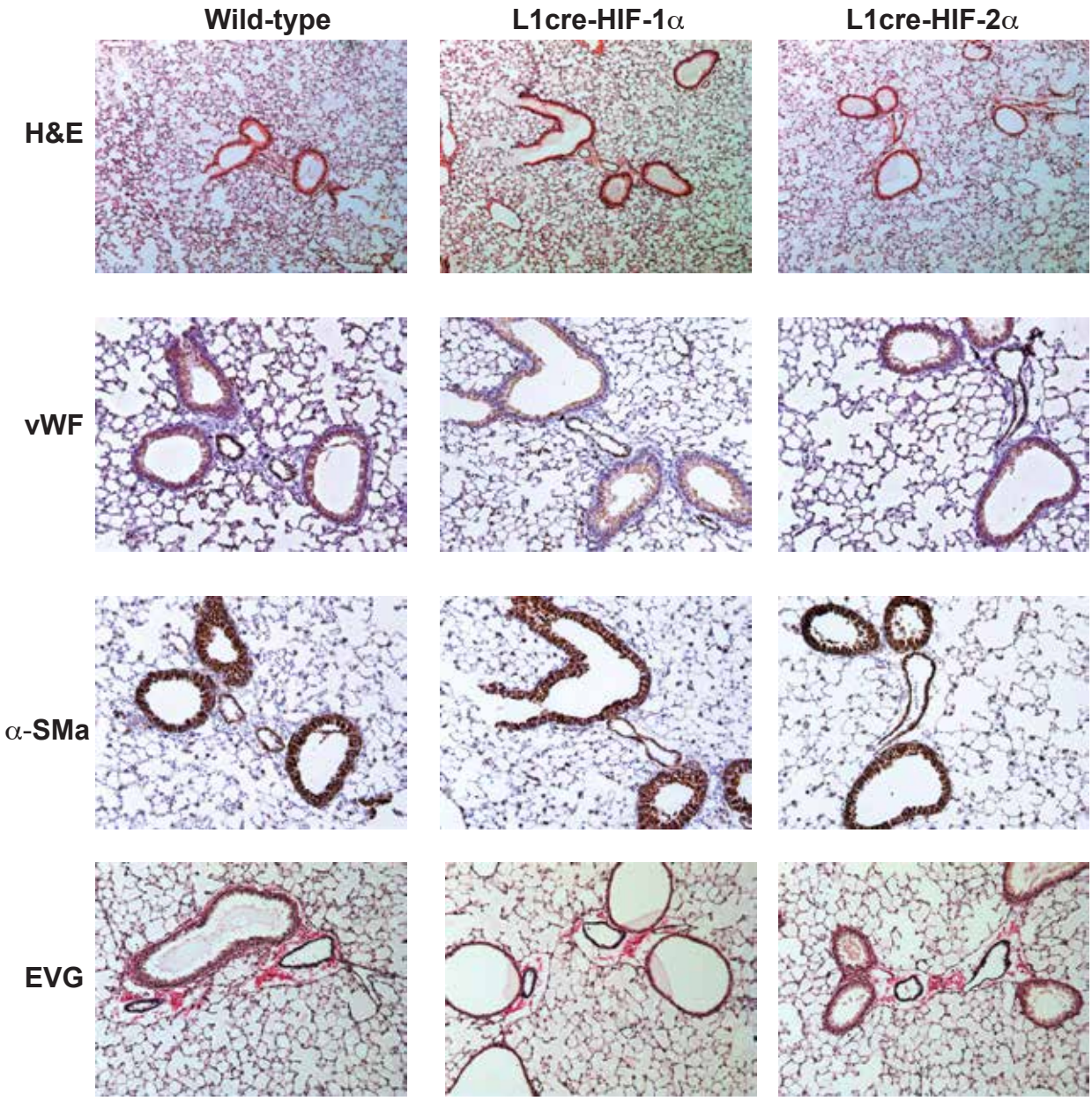

Supplemental Figure 4

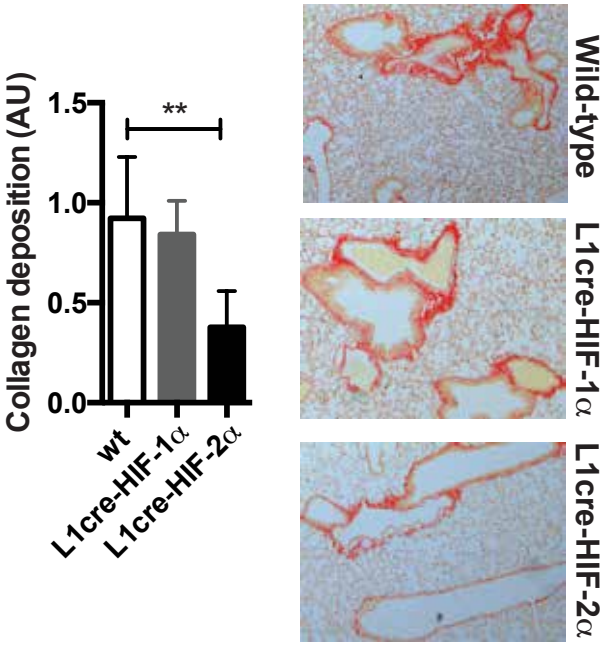

Supplemental Figure 5

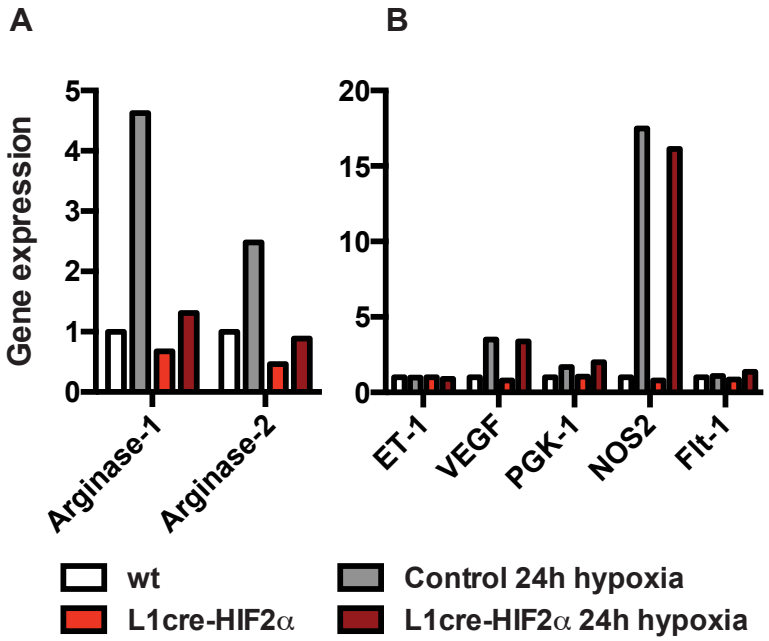

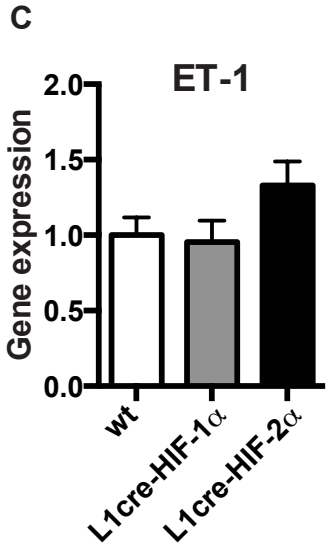

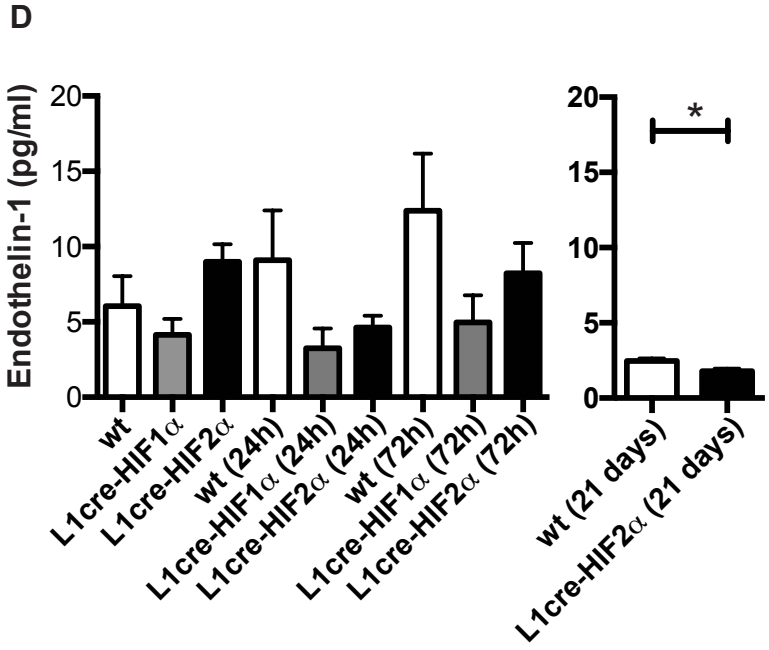

Supplemental Figure 6